

Atmospheric Sulfur Photochemistry on Hot Jupiters

K. Zahnle

NASA Ames Research Center, Moffett Field, CA 94035

`Kevin.J.Zahnle@NASA.gov`

M. S. Marley

NASA Ames Research Center, Moffett Field, CA 94035

`Mark.S.Marley@NASA.gov`

R. S. Freedman

NASA Ames Research Center, Moffett Field, CA 94035

`freedman@darkstar.arc.nasa.gov`

K. Lodders

Washington University - St. Louis

and

J. J. Fortney

Department of Astronomy and Astrophysics, University of California - Santa Cruz

Received _____; accepted _____

submitted to Ap. J. Lett.

ABSTRACT

We develop a new 1D photochemical kinetics code to address stratospheric chemistry and stratospheric heating in hot Jupiters. Here we address optically active S-containing species and CO_2 at $1200 \leq T \leq 2000$ K. HS (mercapto) and S_2 are highly reactive species that are generated photochemically and thermochemically from H_2S with peak abundances between 1-10 mbar. S_2 absorbs UV between 240 and 340 nm and is optically thick for metallicities $[\text{S}/\text{H}] > 0$ at $T \geq 1200$ K. HS is probably more important than S_2 , as it is generally more abundant than S_2 under hot Jupiter conditions and it absorbs at somewhat redder wavelengths. We use molecular theory to compute an HS absorption spectrum from sparse available data and find that HS should absorb strongly between 300 and 460 nm, with absorption at the longer wavelengths being temperature sensitive. When the two absorbers are combined, radiative heating (per kg of gas) peaks at 100 μbars , with a total stratospheric heating of $\sim 8 \times 10^4$ W/m² for a jovian planet orbiting a solar-twin at 0.032 AU. Total heating is insensitive to metallicity. The CO_2 mixing ratio is a well-behaved quadratic function of metallicity, ranging from 1.6×10^{-8} to 1.6×10^{-4} for $-0.3 < [\text{M}/\text{H}] < 1.7$. CO_2 is insensitive to insolation, vertical mixing, temperature ($1200 < T < 2000$), and gravity. The photochemical calculations confirm that CO_2 should prove a useful probe of planetary metallicity.

Subject headings: planetary systems — stars: individual(HD 209458, HD 149026)

1. Introduction

Stratospheric temperature inversions are ubiquitous in the Solar System, and it is beginning to look as if they are commonplace on hot Jupiters as well. Stratospheric temperature inversions form when substantial amounts of light are absorbed at low pressures (high altitudes) where radiative cooling is inefficient. Hubeny et al. (2003) pointed out that efficient absorption of visible light by gaseous TiO and VO would greatly heat the upper atmospheres of those planets already hot enough for these molecules to be present as vapor. Thermal inversions on transiting hot Jupiters were first seen by Richardson et al. (2007) for HD 209458b and Harrington et al. (2007) for HD 149026b. The observed flux ratio at $8\ \mu\text{m}$ for HD 149026b agreed only with models that included a thermal inversion (Fortney et al. 2006). Temperature inversions have since been confirmed by *Spitzer* observations of HD 209458b (Knutson et al. 2008a), XO-1b (Machalek et al. 2008), and TrES-4 (Knutson et al. 2009), all of which show distinctive flux ratios in IRAC bands that suggest inversions (Fortney et al. 2006; Burrows et al. 2007). More circumstantial evidence exists for HD 179949b (Barnes et al. 2008).

On the other hand TrES-1, the least irradiated planet with published *Spitzer* observations, does not appear to have a pronounced inversion (Burrows et al. 2008). Nor, seemingly, does HD 189733b, which is also modestly irradiated (Charbonneau et al. 2008; Barman et al. 2008). One suggestion is that temperature inversions are triggered by irradiation reaching a critical level that is hot enough to evaporate TiO and VO from grains, as discussed by Burrows et al. (2007), Fortney et al. (2008), and Burrows et al. (2008). However, irradiation of XO-1b and HD 189733b is within uncertainties the same (Torres et al. 2008), which poses a challenge to the irradiation trigger.

In the Solar System, stratospheric temperature inversions are often caused by absorption of UV light by gases or aerosols produced by photochemistry. Here we ask if

atmospheric chemistry might play a similar role in hot Jupiters. Speculation has tended to focus on sulfur-containing species (Tinetti 2008), as the reservoir species H_2S is expected to be abundant (Visscher et al 2006) in these atmospheres and many of its breakdown products (S_2 , in particular) absorb violet and ultraviolet light.

2. The Photochemical Model

Previous photochemical modeling of hot Jupiters addressed the abundance of photochemical H (Liang et al 2003) and the absence of photochemical smogs (Liang et al 2004). Liang et al (2003) focused on the high H/ H_2 ratio that arises from H_2O photolysis. In their second paper, Liang et al (2004) argued that simple hydrocarbons would not condense to form photochemical smogs in hot solar composition atmospheres. Neither study considered sulfur.

We have developed a new general purpose 1D photochemical kinetics code applicable to hot extrasolar planets. The code is based on the sulfur photochemistry model for early Earth originally described by Kasting et al (1989) and Kasting (1990), and subsequently adapted by Zahnle et al (2006) and Claire et al (2006) to address sulfur photochemistry of Earth’s atmosphere during the Archean, and by Zahnle et al. (2008) to address martian atmospheric chemistry. Steady state solutions are found by integrating the system through time using a fully implicit backward-difference method.

Our chemical network has been upgraded from that used by Zahnle et al (1995) to address the chemistry generated when the fragments of Comet Shoemaker Levy 9 struck Jupiter. We have assembled a reasonably complete list of the reactions that can take place between the small molecules and free radicals that can be made from H, C, O, N, and S. The code solves 507 chemical reactions for 49 chemical species: H, H_2O , OH, O, O_2 ,

CO, CO₂, HCO, H₂CO, C, CH, CH₂, CH₃, CH₄, CH₃O, C₂, C₂H, C₂H₂, C₂H₃, C₂H₄, C₂H₅, C₂H₆, C₄H, C₄H₂, CN, HCN, N, N₂, NO, NH, NH₂, NH₃, NS, H₂S, HS, S, S₂, S₃, S₄, S₈, SO, HSO, SO₂, OCS, CS, HCS, H₂CS, CS₂, and H₂. Reaction rates, when known, are selected from the publicly available NIST database (<http://kinetics.nist.gov/kinetics>). In order of decreasing priority, we choose between reported reaction rates according to relevant temperature range, newest review, newest experiment, and newest theory. Reverse reaction rates $k_r = K_{\text{eq}}k_f$ of two-body reactions are determined from the forward reaction rate k_f and the equilibrium $K_{\text{eq}} = \exp \{(-\Delta H + T\Delta S) / RT\}$ by using $H^\circ(T)$ and $S^\circ(T)$ as available (R is the gas constant). Rates are not available for all reactions, especially for reactions involving elemental sulfur. We will present a full listing of the chemical reactions important to sulfur in a more general followup study.

Here we use simple descriptions of atmospheric properties. The background atmosphere is 84% H₂ and 16% He. We include Rayleigh scattering by H₂ (Dalgarno and Williams 1962). For our base case we assume an isothermal atmosphere with $T=1400$ K; constant vertical eddy diffusivity $K_{zz} = 1 \times 10^7$ cm²/s; a surface gravity of 20 m/s²; and insolation levels I by a solar twin that are 1000× greater than at Earth. Metallicity proved to be the most interesting parameter and was varied $-0.3 \leq [\text{M}/\text{H}] \leq 1.7$. In these units, solar metallicity is $[\text{M}/\text{H}] = 0$, Jupiter’s is $[\text{M}/\text{H}] = 0.5$, and Saturn’s is $[\text{M}/\text{H}] = 0.8$. Short chemical lifetimes of S-containing species make our results insensitive to K_{zz} . Model parameters are listed in Table 1.

At the upper boundary we set a zero flux lid at 1 μ bar, with neither escape nor exogenous supply. For the lower boundary we use fixed equilibrium mixing ratios of the most abundant species at 1 bar of H₂ and temperature T (Lodders and Fegley 2002, Visscher et al 2006). For other species we force the mixing ratio at 1 bar to approach zero. We scale the lower boundary conditions such that the total mixing ratios of C, O, N, and S

all scale linearly with metallicity.

Absorption by S_2 between 240 nm and ~ 360 nm from the ground state is analogous to the Schumann-Runge system in O_2 (Okabe 1978). Strong, distinctive S_2 emission near 300 nm was observed on Jupiter after the impact with Shoemaker-Levy 9 with Jupiter in 1994 (Noll et al 1995). Subsequent thermochemical modeling showed that S_2 readily forms as a major product in a shock-heated ($T > 1000$ K) gas of either cometary or jovian composition (Zahnle et al 1995, Zahnle 1996). S_2 has also been seen in gases vented by volcanoes on Io (Spencer et al, 2000; Moses et al 2002). For S_2 , we use absorption cross sections at 1500 K computed by van der Heijden and van der Mullen (2001).

The HS (mercapto) radical absorbs from its ground state at 324 nm (Okabe 1978). Visscher et al (2006) predicted that HS would be very abundant in equilibrium at hot Jupiter conditions. We find the same. We therefore calculated absorption cross sections of HS at four temperatures at 30 mbar pressure using literature values of the molecular properties. The ground $X^2\Pi$ state has been well studied (Ram et al 1995) but the upper level $A^2\Sigma^+$ is subject to strong pre-dissociation (Resende and Ornellas 2001, Wheeler et al 1997, Schneider et al 1990, Henneker and Popkie 1971), and only the value of the rotational constant B and the spacing of the lowest vibrational energy levels have been well measured. Using these constants and a value for the electronic band oscillator strength of the 0-0 transition derived from a study of HS in the solar spectra by Berdyugina and Livingston (2002), a line list was computed using the RLS code developed by R.N. Zare and D. Albritton (Zare et al 1973). This RLS code uses the molecular constants and band strengths to predict line positions and strengths by fitting to an RKR potential (Zare et al 1973). Other needed data — Franck-Condon factors, partition functions, etc. — were derived either from the cited literature, the program itself, or from Sauval and Tatum (1984) or Larsson (1983). The calculations were carried out for values of $v''(0-4)$ and $v'(012)$. Because

the excited vibrational levels of the $A^2\Sigma^+$ state are unstable with respect to predissociation, the corresponding optical transitions are likely to be broad and shallow, or even continuous. These uncertainties principally affect the absorption spectrum at wavelengths shorter than 324 nm, which is in the range that is absorbed strongly by S_2 . Results are shown in Figure 1. In the photochemical model we used only the 1500 K absorption coefficients.

Other sulfur allotropes are better absorbers than S_2 but less abundant. S_3 absorbs strongly between 350 and 500 nm, and S_4 absorbs between 450 nm and 600 nm, but more weakly (Billmers and Smith 1991). Unfortunately, the chemistries of S_3 and S_4 are very uncertain, and we have had to estimate the important reaction rates. In an earlier version of this study, we focused on the heats of formation, and we tentatively concluded that S_3 heating would be important for metallicities $[S/H] > 0.7$. We have since learned that reactions of the form $H + S_n \rightarrow HS + S_{n-1}$, where $n \geq 2$, are strongly favored by entropy. The revised model predicts less S_2 and much less S_3 , which reduces the importance of S_3 heating considerably.

Sulfanes (H_2S_n , hydropolysulfides) will be present in cooler hot Jupiters. At low temperatures sulfanes absorb VUV between 260 nm and 330 nm (Steudel and Eckert 2003). Absorption may extend beyond 400 nm at higher temperatures as the ground state becomes vibrationally excited, as in HS, but to first approximation these wavelengths are covered by the more abundant S_2 and HS. We have not included sulfanes in this study.

3. Results

Figure 2 shows how CO_2 and the abundant S-containing species vary as a function of altitude. This particular case shows a hot Jupiter at 1400 K with a “planetary” metallicity of $[M/H] = 0.7$. Figure 2 is broadly representative of all our models with $1200 \leq T \leq 2000$

K and $-0.3 < [M/H] < 1.7$. In particular, S_2 and HS show well-defined peaks at ~ 2 mbars that coincide with the altitude where H_2S photolysis becomes important. At lower altitudes H_2S is the main S-containing species, and at higher altitudes S is. It is also notable that the atmosphere becomes more oxidizing at higher altitudes where H_2O photolysis is important.

Table 1 lists some key results pertinent to sulfur for several variations of basic model parameters. The models assume that $K_{zz} = 10^7 \text{ cm}^2/\text{s}$ and $g = 2000 \text{ cm/s}^2$ unless otherwise noted. In this temperature range the models are insensitive to K_{zz} (results not shown). Model G shows that, as expected, column densities vary inversely with g .

Column densities of S_2 and HS are sensitive to metallicity. To first approximation, species with one metal atom, such as H_2O and H_2S , increase linearly with metallicity, and species with two metal atoms, such as SO and S_2 , increase as the square of metallicity (Visscher et al 2006). A slight complication is that CO and N_2 increase linearly with metallicity because these are the major reservoir species for C and N, respectively; hence CO_2 increases as the square of metallicity (as $CO \times O$), rather than as the cube.

The models are not sensitive to temperature and insolation over the parameter ranges ($1200 \leq T \leq 2000 \text{ K}$ and $1 \leq I \leq 1000$) presented here. Insensitivity of the chemistry to T and I surprised us, and suggests that thermochemical equilibrium is more important for sulfur than photochemistry or kinetics. Minor differences are that HS is favored by higher temperatures and SO and S_2 are favored by high I . Not shown here is that the chemistry changes markedly for $T < 1100 \text{ K}$: hydrocarbons, CS, and CS_2 become abundant, and the results become sensitive to K_{zz} . Cooler atmospheres introduce a variety of new topics best left for another study.

Carbon dioxide, a robust molecule and a potential observable, has been reported in HD 189733b by Swain et al (2009). CO_2 is generated from CO by reaction with OH radicals. The chief source of OH is the reaction of H_2O with atomic hydrogen; at high

altitudes UV photolysis of H_2O is also important. We find that CO_2 mixing ratios range from 1.6×10^{-8} to 1.6×10^{-4} for $-0.3 \leq [M/H] \leq 1.7$, scaling as the square of metallicity. Table 1 lists computed CO_2 mixing ratios in the models discussed here. These results are insensitive to insolation, vertical mixing, temperature between 1200 K and 2000 K, and gravity. The CO_2/CO ratio is nearly independent of pressure, as seen in Figure 2. Pressure independence is expected because the controlling reactions, $\text{CO}_2 + \text{H} \leftrightarrow \text{CO} + \text{OH}$ and $\text{H} + \text{H}_2\text{O} \leftrightarrow \text{H}_2 + \text{OH}$, and the controlling equilibrium, $\text{CO}_2 + \text{H}_2 \leftrightarrow \text{CO} + \text{H}_2\text{O}$, all leave the total pressure unchanged. (At very high altitudes photochemistry alters the CO_2/CO ratio.) The computed CO_2 abundances are in good agreement with the reported observation of CO_2 at the ppmv level in HD 189733b (Swain et al. 2009). The sensitivity of CO_2 to metallicity and insensitivity to other atmospheric parameters makes CO_2 a good probe of planetary metallicity, as pointed out by Lodders and Fegley (2002).

3.1. Optical depth and stratospheric heating

Figure 3 shows the pressure levels where the solar and planetary metallicity atmospheres of Models A, M, and MM become optically thick. Opacity is dominated by HS, with some contribution by S_2 at wavelengths shorter than 300 nm. The twin peaks between 300 nm and 320 nm may be fictitious, but the peak at 324 nm could prove diagnostic of HS. A solar and a K0V stellar spectrum are shown for comparison.

Figure 4 shows the magnitude of stratospheric heating and the pressure level where the heating occurs for a solar-twin primary at 0.032 AU ($I = 1000$) for 3 metallicities (Models A, M, and MM). Radiative heating is dominated by HS, and is nearly saturated through the stratosphere for all these models (see also Table 1). By contrast, peak heating at $\sim 100 \mu\text{bars}$ takes place where SO and SO_2 are significant. The sensitivity of SO and SO_2 to metallicity is reflected in greater heating rates at $\sim 100 \mu\text{bars}$.

Cumulative stratospheric heating rates for these models are listed in Table 1. For a solar-twin at 0.032 AU, cumulative heating above 1 mbar is typically 4×10^4 W/m² and above 0.1 bars is typically 8×10^4 W/m², i.e., about half the energy is absorbed in the lower stratosphere. Burrows et al. (2008) modeled hot stratospheres by adding an unknown gray absorber. They found that gray cross-sections of $0.05 - 0.6$ cm²/g, averaged over 430 to 1000 nm for altitudes above 0.03 bars, could produce the observed heating. Heating profiles using gray opacities in this range are plotted for comparison on Fig 4 for the same planet and star. The gray opacities produce more heating in total (indeed, the stratospheres in both these models are optically thick), and more heating at low altitudes, but at higher altitudes sulfur generates heating at levels quite similar to what Burrows et al find useful.

4. Conclusions

We develop a new 1D photochemical model for stratospheric modeling of hydrogen-rich atmospheres of warm or hot exoplanets. This model is applicable to any H-rich planet subject to high insolation, including hot Neptunes, superearths, and waterworlds. Here we apply the model to sulfur chemistry, stratospheric heating, and CO₂ abundance.

We find that hot stratospheres of hot Jupiters could be explained by absorption of UV and violet visible light by HS and S₂, two highly reactive species that are generated chemically from H₂S. For a hot Jupiter orbiting a solar-twin at 0.032 AU, for a wide range of possible planetary compositions, HS and S₂ together absorb 4×10^4 W/m² at altitudes above 1 mbar and another 4×10^4 W/m² at altitudes between 1 mbar and 0.1 bar. This level of heating approaches what Fortney et al (2006) and Burrows et al (2008) use in their most successful LTE spectral models. Non-LTE mechanisms may improve the agreement, because LTE models systematically overestimate radiative cooling and thus underestimate the temperature. Chemiluminescence by H₂O, formed by the exothermic reaction of

OH+H₂, might also be expected.

Although our computed HS and S₂ column densities increase with metallicity, optically thick columns are predicted for all plausible atmospheric compositions, which means that millibar-level temperature inversions are expected to be commonplace. The distinctive interaction of S₂ and HS with near ultraviolet light could make these species detectable in transit by the refurbished HST; there is evidence for a blue absorber in legacy HST data of HD 209458b (Sing et al 2008).

On the other hand, sulfur does not give an easy answer to why some hot Jupiters have superheated stratospheres, and others not. In an earlier draft of this study, we speculated that S₃—which is very sensitive to metallicity—might be part of the explanation. This no longer appears likely. We have since developed a better understanding of HS’s opacity, which turns out to be considerable. We no longer see a strong connection between metallicity and radiative heating, save at very low pressures ($< 100\mu\text{bars}$) where SO and SO₂ become important. It now seems that sulfur chemistry by itself is unlikely to explain differences between planets, although planetary metallicity may still be key.

Heating by sulfur compounds does not preclude heating by TiO and VO on hotter planets. Sulfur species provide considerable heating from below 1000 K to above 2000 K, but they do not provide the spectral coverage at visible wavelengths that TiO and VO provide. For TiO and VO to be abundant enough to explain stratospheric heating, the temperature needs to be very high, in excess of 2000 K, and not just in the stratosphere but also at deeper levels in the planet where these two refractory oxides would otherwise be cold-trapped in silicate clouds. OGLE-TR-56b (Sing and López-Morales 2009) seems to meet the TiO-VO threshold.

CO₂ is generated by the reaction of CO with OH and destroyed by the reverse (endothermic) reaction with H, $\text{CO} + \text{OH} \leftrightarrow \text{CO}_2 + \text{H}$. At low altitudes OH is generated

by the reaction of H_2O with atomic H, supplemented at high altitudes by UV photolysis of H_2O . As both the major source and major sink of CO_2 are proportional to atomic hydrogen densities, the kinetic inhibition against hydrogen recombination does not disturb CO_2 's thermochemical equilibrium. We find that CO_2 mixing ratios vary quadratically with metallicity from 1.6×10^{-8} to 1.6×10^{-4} for $0 < [\text{M}/\text{H}] < 0.7$. This result is insensitive to insolation, vertical mixing, temperature (for $1200 \leq T \leq 2000$ K), and gravity. Because the reactions that form and destroy CO_2 leave the total number of molecules unchanged, the CO_2/CO ratio is also pressure independent. The computed CO_2 abundances are in good agreement with the observation of CO_2 at the ppmv level in HD 189733b (Swain et al 2009). Therefore we confirm Lodders and Fegley's (2002) suggestion that CO_2 is a promising probe of planetary metallicity.

5. Acknowledgements

We thank R. V. Yelle for discussions regarding the potential importance of S_3 , and G. Tinetti for an insightful review. We thank NASA's Exobiology and Planetary Atmospheres Programs for support. KL was also supported by NSF Grant AST-0707377.

REFERENCES

- Allard, F., Hauschildt, P. H., Alexander, D. R., Tamanai, A., & Schweitzer, A. 2001, *ApJ*, 556, 357
- Barman, T. S. 2008, *ApJ*, 676, L61
- Barnes, J. R., Barman, T. S., Jones, H. R. A., Leigh, C. J., Cameron, A. C., Barber, R. J., & Pinfield, D. J. 2008, *MNRAS*, 390, 1258
- Berdyugina, S.V. and Livingston, W.C. (2002) *Astron. Astrophys.* 387, L6-L9.
- Billmers RI and Smith AL (1991). *J. Phys. Chem.* 95, 4242-4245.
- Burrows, A., Hubeny, I., Budaj, J., Knutson, H. A., & Charbonneau, D. 2007, *ApJ*, 668, L171
- Burrows, A., Budaj, J., & Hubeny, I. 2008, *ApJ*, 678, 1436
- Burrows, A., Budaj, J., & Hubeny, I. 2008, *ApJ*, 678, 1436
- Charbonneau, D., Knutson, H. A., Barman, T., Allen, L. E., Mayor, M., Megeath, S. T., Queloz, D., & Udry, S. 2008, *ApJ*, 686, 1341
- Claire MW, Catling DC, Zahnle KJ (2006). *Geobiology* 4, 239-269.
- Dalgarno A and Williams DA (1962). . *Astrophys. J.* 136, 690-692.
- Désert, J.-M., Vidal-Madjar, A., Lecavelier Des Etangs, A., Sing, D., Ehrenreich, D., Hébrard, G., & Ferlet, R. 2008, *A&A*, 492, 585
- Fegley, B. J. & Lodders, K. 1994, *Icarus*, 110, 117
- Fortney, J. J., Saumon, D., Marley, M. S., Lodders, K., & Freedman, R. S. 2006, *ApJ*, 642, 495
- Fortney, J. J., Lodders, K., Marley, M. S., & Freedman, R. S. 2008, *ApJ*, 678, 1419
- Harrington, J., Luszcz, S., Seager, S., Deming, D., & Richardson, L. J. 2007, *Nature*, 447, 691

- Henneker, W. H. and Popkie, H.E. (1971) *J. Chem. Phys.* **54**, 1763-1778.
- Hubeny, I., Burrows, A., & Sudarsky, D. 2003, *ApJ*, **594**, 1011
- Kasting JF, Zahnle KJ, Pinto JP, Young AT (1989) *Origins of Life*, **19**, 95-108.
- Kasting JF (1990). *Origins of Life* **20**, 199-231.
- Knutson, H. A., Charbonneau, D., Allen, L. E., Burrows, A., & Megeath, S. T. 2008, *ApJ*, **673**, 526
- Knutson, H. A., Charbonneau, D., Burrows, A., O’Donovan, F. T., & Mandushev, G. 2009, *ApJ*, **691**, 866
- Larsson, M. (1983) *Astron. Astrophys.* **128**, 291-298.
- Liang M-C, Parkinson CD, Lee AYT, Yung YL, and Seager S, (2003) “Source of atomic hydrogen in the atmosphere of HD 209458b” *Astrophys. J.* **596**, L247L250.
- Liang M-C, Seager S, Parkinson CD, Lee AYT, and Yung YL (2004) “On the insignificance of photochemical hydrocarbon aerosols in the atmospheres of close-in extrasolar giant planets” *Astrophys. J.* **605**, L61L64.
- Lodders, K. and Fegley B. (1999) *The Planetary Scientist’s Companion*. Oxford.
- Lodders, K. 1999, *ApJ*, **519**, 793
- . 2002, *ApJ*, **577**, 974
- Lodders, K. and Fegley, B.J. (2002). *Icarus* **155**, 393-424.
- Machalek P, McCullough PR, Burke CJ, Valenti JA, Burrows A, and Hora JL (2008) *Astrophys. J.* **684**, 1427-1432.
- Marley, M. S., Fortney, J., Seager, S., & Barman, T. 2007, in *Protostars and Planets V*, ed. B. Reipurth, D. Jewitt, & K. Keil, 733–747

- Moses JI, Zolotov MY, and Fegley B (2002). *Icarus* 156, 76106.
- Nicholas, J.E., Amodio, C.A., Baker, M.J. (1979) *J. Chem. Soc. Faraday Trans. 1*:75, 1868-1880.
- Noll KS, McGrath MA, Trafton LM, Atreya SK, Caldwell JJ, Weaver HA, Yelle RV, Barnet C, and Edgington S (1995) *Science*, 267, 1307.
- Okabe H (1978) *The Photochemistry of Small Molecules*. Wiley-Interscience, New York, 431 pp.
- Ram, R S, Bernath P. F., Engleman R. and Brault J. W. (1995) *J. Molec. Spect.* 172, 34-42.
- Resende, S.M., and Ornellas, F.R. (2001) *J. Chem. Phys.* 115, 2178-2187.
- Richardson, L. J., Deming, D., Horning, K., Seager, S., & Harrington, J. 2007, *Nature*, 445, 892
- Sauval, A.J. and Tatum, J.B. (1984) *Astrophys. J. Supp.* 56, 193-209.
- Schneider, L., Meier W, and Weige KH (1990) *J. Chem. Phys.* 92, 7027-7037.
- Showman, A. P., Fortney, J. J., Lian, Y., Marley, M. S., Freedman, R. S., Knutson, H. A., & Charbonneau, D. 2008, ArXiv e-prints
- Sing, D.K., Vidal-Madjar A., Désert, J.-M., Lecavelier des Etangs, A., and Ballester, G. (2008). *Astrophys. J.* 686, 658-666.
- Sing, D.K., and López-Morales, M. (2009). *Astron. Astrophys.* 493, L31-L34.
- Spencer JR., Jessup, KL, McGrath MA, Ballester GE, amd Yelle RV (2000). *Science* 288, 1208-1210.
- Steudel R and Eckert B (2003). *Elemental sulfur and sulfur-rich compounds*. Springer, 202 pp.
- Swain, M. R., Vasisht, G., Tinetti, G., Bouwman, J., Chen, P., Yung, Y., Deming, D., & Deroo, P. 2009, *Astrophys. J. Lett.* 690, L114-L117.
- Tinetti, G. (2008). *Bull. Am. Astron. Soc.* 40, 463.
- Torres, G., Winn, J. N., & Holman, M. J. 2008, *ApJ*, 677, 1324

- van der Heijden and van der Mullen (2001). *J. Phys. B. Atom. Mol. Opt. Phys.* *34*, 4183-4201.
- Visscher C, Lodders K, and Fegley B. (2006). *Astrophys. J.* *648*, 1181-1195.
- Wheeler, M.D., Orr-Ewing, AJ, and Ashfold, MNR (1997) *J. Chem. Phys.* *107*, 7591-7600.
- Zahnle KJ, Mac Low M-M, Lodders K, and Fegly B. (1995). *Geophys. Res. Lett.* *22*, 1593-1596.
- Zahnle KJ, Claire MW, Catling DC (2006). *Geobiology* *4*, 271-282.
- Zahnle KJ, Haberle RM, Catling DC, Kasting JF (2008). *J. Geophys. Res.* *113*, E11004,
doi:10.1029/2008JE003160.
- Zare, R.N., Schmeltekopf AL, Harrop WJ, and Albritton DL (1973) *J. Molec. Spect.* *46*, 37-66.

Model	[M/H] ^a	<i>I</i> ^b	<i>T</i>	S ₂ [cm ^{−2}] ^c	HS [cm ^{−2}] ^c	HS ^d	SO ^d	CO ₂ ^d	Heating ^e	Heating ^f
A	0	1000	1400	4.2×10^{18}	1.2×10^{20}	6	0.07	0.065	6.4×10^4	2.7×10^4
M	0.7	1000	1400	2.2×10^{20}	1.0×10^{21}	26	1.7	1.6	8.4×10^4	4.1×10^4
MM	1.4	1000	1400	6.0×10^{21}	5.4×10^{21}	100	27	41	1.1×10^5	5.1×10^4
H	0.7	1000	1600	2.2×10^{20}	2.3×10^{21}	43	1.2	1.4	9.0×10^4	4.3×10^4
HH	0.7	1000	1800	1.9×10^{20}	4.0×10^{21}	52	1.3	1.5	9.5×10^4	4.4×10^4
HHH	0.7	1000	2000	1.3×10^{20}	5.0×10^{21}	41	1.4	1.3	9.6×10^4	4.1×10^4
C	0.7	1000	1200	1.6×10^{20}	2.5×10^{20}	11	1.9	1.9	7.5×10^4	3.7×10^4
G	0.7	1000	1400	4.3×10^{20}	2.0×10^{21}	32	1.3	1.6	9.3×10^4	4.7×10^4
I	0.7	200	1400	2.1×10^{20}	1.0×10^{21}	37	0.9	1.6	1.7×10^4	8.8×10^3
SSC	0.7	1	1200	1.1×10^{20}	2.4×10^{20}	16	0.06	1.9	72	44

a – Metallicity. This notation means that the planet is 10^[M/H] richer in C, S, N, and O than the Sun.

b – Insolation. *I* = 1000 corresponds to a solar twin primary at 0.032 AU.

c – Column densities above 1 bar.

d – Mixing ratio in ppmv at 1 mbar.

e – Total atmospheric heating [W/m²] above 0.1 bar for a solar twin source.

f – Total atmospheric heating [W/m²] above 1 mbar for a solar twin source.

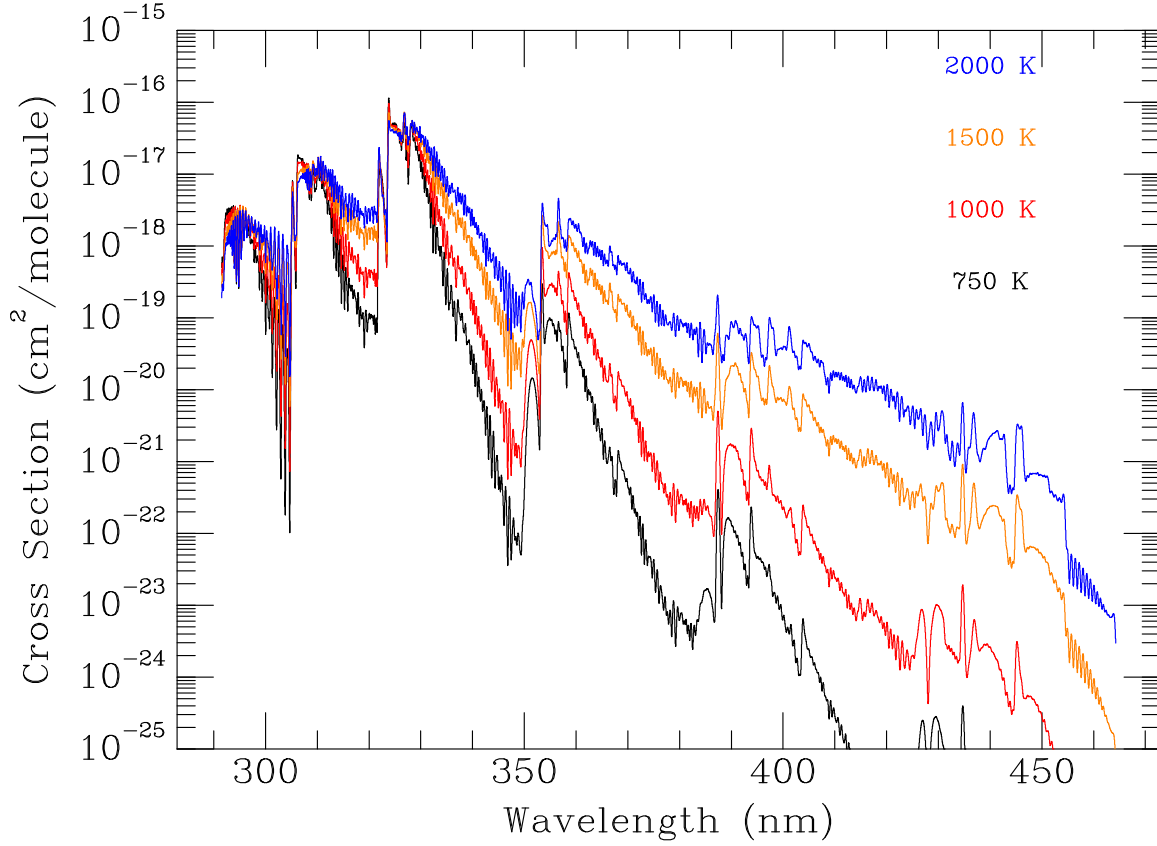


Fig. 1.— Theoretical absorption cross sections of HS radicals at near UV, violet and indigo wavelengths at four temperatures at 30 mbar pressure. Cross sections were computed from the lowest five vibrational levels of the ground electronic state $X^2\Pi$ to the lowest three vibrational levels of the upper level $A^2\Sigma^+$. The excited vibrational levels of $A^2\Sigma^+$ are strongly predissociating, which suggests that absorption at wavelengths shorter than 324 nm is probably continuous rather than allocated into the well-defined bands shown here.

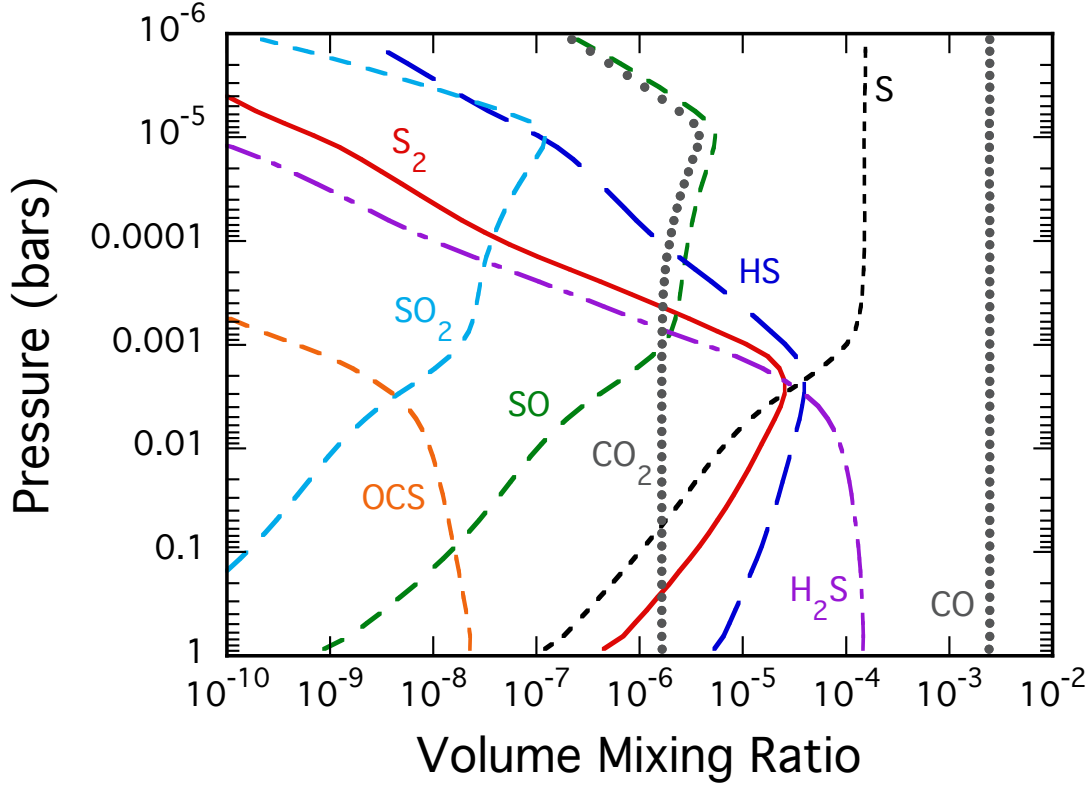


Fig. 2.— Important sulfur species, CO, and CO₂ in the atmosphere of a hot Jupiter with a “planetary” metallicity of $[M/H] = 0.7$. The atmosphere is assumed isothermal at 1400 K and insolated 1000× more strongly than Earth. Other model M parameters are listed in Table 1. The prominent transition at ~ 2 mbar — where the S₂ mixing ratio peaks — is associated with photolysis of H₂S. The bump in CO₂ at 6 μ bars is attributable to photochemistry. Abundance profiles in the 1400 K atmosphere are generally representative of atmospheres with $1200 \leq T \leq 2000$ K.

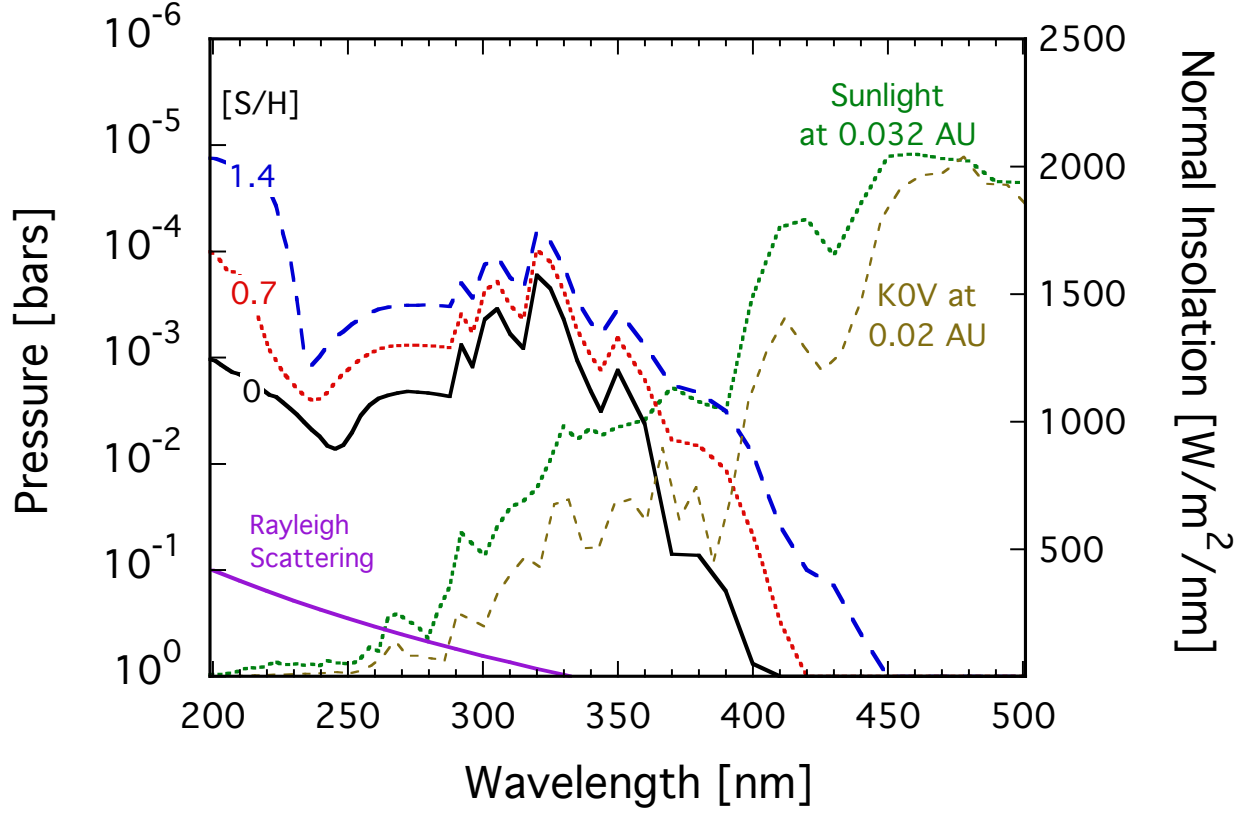


Fig. 3.— Pressure levels of the $\tau = 1$ surface as a function of wavelength for three metallicities, $[S/H] = 0, 0.7$, and 1.4 . These metallicities correspond to models A, M, and MM of Table 5. Absorption between 250 and 300 nm is mostly by S_2 and absorption between 300 and 460 nm is by HS. Structure blueward of 324 nm is associated with transitions to predissociating states and is probably fictitious. The $\tau = 1$ surface of a pure H_2 Rayleigh scattering atmosphere and two incident stellar spectra, one for the Sun and another for a generic K0V dwarf, are shown for comparison.

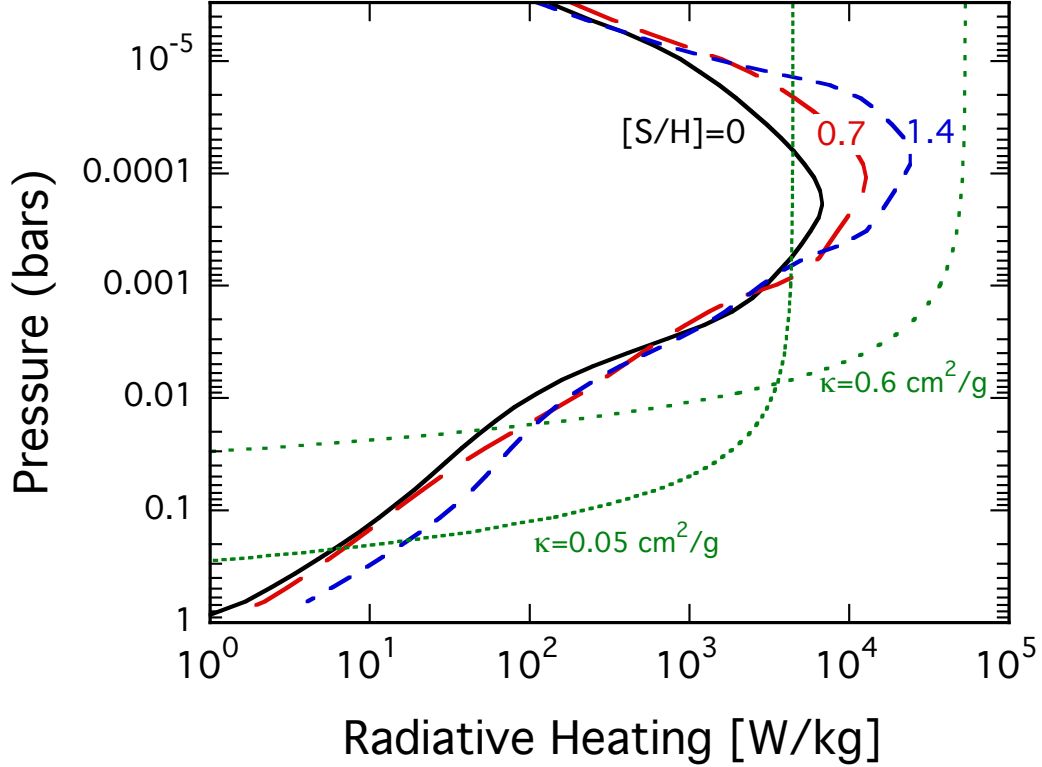


Fig. 4.— Radiative heating at different altitudes for three metallicities, $[S/H] = 0, 0.7,$ and 1.4 . These correspond to models A, M, and MM of Table 5. Heating rates are given in W/kg, which emphasizes the potential impact on temperature. Heating peaks at $100 \mu\text{bars}$ but extends through the stratosphere. Heating with constant gray opacities of 0.05 and $0.6 \text{ cm}^2/\text{g}$ for $430 < \lambda < 1000 \text{ nm}$ is shown for comparison.